



Nickel-hydrogen batteries for large-scale energy storage

Wei Chen^a, Yang Jin^a, Jie Zhao^a, Nian Liu^{b,1}, and Yi Cui^{a,c,2}

^aDepartment of Materials Science and Engineering, Stanford University, Stanford, CA 94305; ^bDepartment of Chemistry, Stanford University, Stanford, CA 94305; and ^cStanford Institute for Materials and Energy Sciences, SLAC National Accelerator Laboratory, Menlo Park, CA 94025

Edited by Peidong Yang, University of California, Berkeley, and approved September 26, 2018 (received for review June 1, 2018)

Large-scale energy storage is of significance to the integration of renewable energy into electric grid. Despite the dominance of pumped hydroelectricity in the market of grid energy storage, it is limited by the suitable site selection and footprint impact. Rechargeable batteries show increasing interests in the large-scale energy storage; however, the challenging requirement of low-cost materials with long cycle and calendar life restricts most battery chemistries for use in the grid storage. Recently we introduced a concept of manganese-hydrogen battery with Mn²⁺/MnO₂ redox cathode paired with H⁺/H₂ gas anode, which has a long life of 10,000 cycles and with potential for grid energy storage. Here we expand this concept by replacing Mn²⁺/MnO₂ redox with a nickel-based cathode, which enables ~10× higher areal capacity loading, reaching ~35 mAh cm⁻². We also replace high-cost Pt catalyst on the anode with a low-cost, bifunctional nickel-molybdenum-cobalt alloy, which could effectively catalyze hydrogen evolution and oxidation reactions in alkaline electrolyte. Such a nickel-hydrogen battery exhibits an energy density of ~140 Wh kg⁻¹ (based on active materials) in aqueous electrolyte and excellent rechargeability with negligible capacity decay over 1,500 cycles. The estimated cost of the nickel-hydrogen battery based on active materials reaches as low as ~\$83 per kilowatt-hour, demonstrating attractive characteristics for large-scale energy storage.

battery | large-scale energy storage | hydrogen catalysts | nickel-hydrogen | nickel-molybdenum-cobalt

For renewable energy resources such as wind and solar to be competitive with traditional fossil fuels, it is crucial to develop large-scale energy storage systems to mitigate their intrinsic intermittency (1, 2). The cost (US dollar per kilowatt-hour; \$ kWh⁻¹) and long-term lifetime are the utmost critical figures of merit for large-scale energy storage (3–5). Currently, pumped-hydroelectric storage dominates the grid energy storage market because it is an inexpensive way (~\$100 kWh⁻¹) to store large quantities of energy (accounts for more than 95% of global storage capacity) over a long period of time (~50 y), but it is restricted by the lack of suitable sites and the environmental footprint (6). Other technologies such as compressed air and flywheel energy storage show some advantages for grid storage, but their relatively low efficiency and high cost need to be significantly improved (7). Rechargeable batteries offer great opportunities to target low-cost, high capacity, and highly reliable systems for large-scale energy storage (3). Representatives of the battery technologies include lead-acid (8), redox-flow (9), lithium-ion (10), sodium-sulfur (11), and liquid-metal (12); however, these existing technologies can hardly fulfill the overall economic requirements for the large utility market due to a variety of unsolved issues (2, 4, 7). Historically, conventional nickel-hydrogen battery shows outstanding rechargeability without capacity decay for over 30,000 cycles, which has been applied extensively in aerospace such as satellites and aircraft with service life of more than three decades due to its high reliability, stability, and durability (13). However, the utilization of costly Pt catalysts in the conventional nickel-hydrogen battery impedes its widespread applications. The attractive characteristics of the conventional nickel-hydrogen battery inspire us to explore

advanced nickel-hydrogen battery with low cost to achieve the United States Department of Energy (DOE) target of \$100 kWh⁻¹ for grid storage (14), which is highly desirable yet very challenging.

Recently we demonstrated a battery chemistry of manganese-hydrogen (Mn-H), where the cathode is cycled between soluble Mn²⁺ and solid MnO₂ and the anode is cycled between H⁺ and H₂ gas through the well-known hydrogen evolution and oxidation reactions (HER and HOR) on a Pt electrocatalyst. Such a hydrogen battery concept represents promises of high energy density, fast charge-discharge rate capability, and long-term cycle stability. However, the areal capacity of the Mn-H battery still needs improvement due to the limited mass loading of the MnO₂ on the cathode. The utilization of expensive Pt electrocatalyst in the Mn-H battery calls for low-cost alternatives. Here we expand this battery chemistry to nickel-hydrogen (Ni-H), where the cathode is replaced by the nickel-based electrode with high areal capacity and the anode electrocatalyst is replaced by low-cost, earth-abundant, bifunctional HER/HOR electrocatalyst of nickel-molybdenum-cobalt (NiMoCo), addressing the challenges of the Mn-H battery and exhibiting great promise for practical large-scale energy storage.

The fabrication and energy storage mechanism of the Ni-H battery is schematically depicted in Fig. 1A. It is constructed in a custom-made cylindrical cell by rolling Ni(OH)₂ cathode, polymer separator, and NiMoCo-catalyzed anode into a steel vessel, similar to the fabrication of commercial AA batteries. The cathode nickel hydroxide/oxyhydroxide (Ni(OH)₂/NiOOH) reaction is known to be highly rechargeable for commercial alkaline batteries including

Significance

Rechargeable batteries offer great opportunities to target low-cost, high-capacity, and highly reliable systems for large-scale energy storage. This work introduces an aqueous nickel-hydrogen battery by using a nickel hydroxide cathode with industrial-level areal capacity of ~35 mAh cm⁻² and a low-cost, bifunctional nickel-molybdenum-cobalt electrocatalyst as hydrogen anode to effectively catalyze hydrogen evolution and oxidation reactions in alkaline electrolyte. The nickel-hydrogen battery exhibits an energy density of ~140 Wh kg⁻¹ in aqueous electrolyte and excellent rechargeability without capacity decay over 1,500 cycles. The estimated cost of the nickel-hydrogen battery reaches as low as ~\$83 per kilowatt-hour, demonstrating attractive potential for practical large-scale energy storage.

Author contributions: W.C. and Y.C. designed research; W.C., Y.J., J.Z., and N.L. performed research; W.C. analyzed data; and W.C. wrote the paper.

Conflict of interest statement: We are applying for a patent on this work.

This article is a PNAS Direct Submission.

Published under the PNAS license.

¹Present address: School of Chemical and Biomolecular Engineering, Georgia Institute of Technology, Atlanta, GA 30332.

²To whom correspondence should be addressed. Email: yicui@stanford.edu.

This article contains supporting information online at www.pnas.org/lookup/suppl/doi:10.1073/pnas.1809344115/-DCSupplemental.

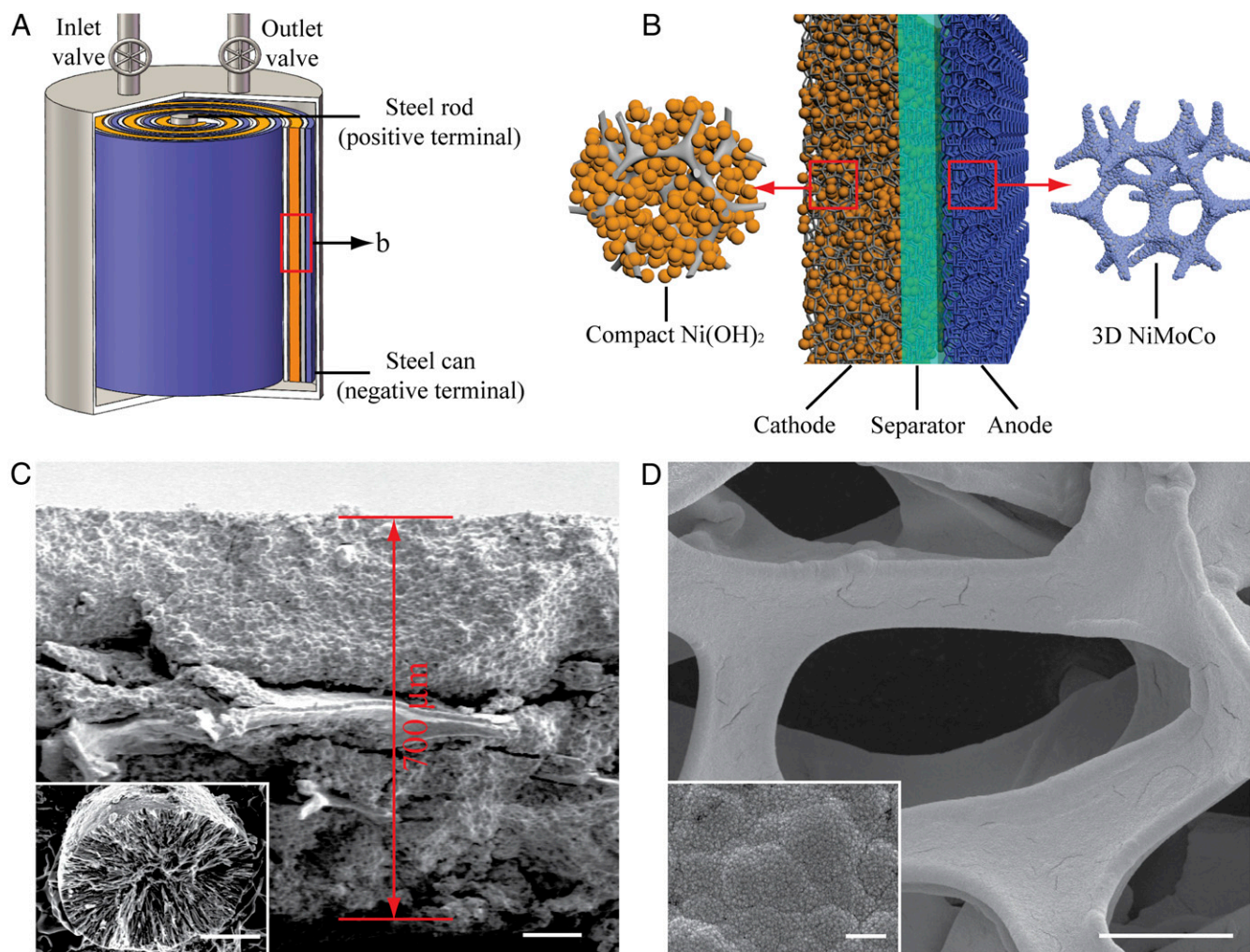


Fig. 1. The Ni-H cylindrical battery. (A) Schematic of the Ni-H cylindrical battery design. (B) Electrode configuration and specification of the Ni-H battery. (C) A cross-sectional SEM image shows that the thickness of the cathode is $\sim 700 \mu\text{m}$. (Scale bar: $100 \mu\text{m}$.) (Inset) An SEM image shows that the cathode comprises $\text{Ni}(\text{OH})_2$ microspheres. (Scale bar: $5 \mu\text{m}$.) The compact $\text{Ni}(\text{OH})_2$ cathode has a high tap density of $\sim 2.6 \text{ g cm}^{-3}$ and a mass loading of $\sim 182 \text{ mg cm}^{-2}$ with respect to the active $\text{Ni}(\text{OH})_2$. (D) An SEM of the 3D NiMoCo anode. (Scale bar: $100 \mu\text{m}$.) (Inset) An SEM image shows the NiMoCo nanoparticles on the nickel foam. (Scale bar: $1 \mu\text{m}$.) The NiMoCo anode has a thickness of $\sim 200 \mu\text{m}$.

nickel-cadmium, nickel-hydrogen, and nickel-metal hydrides (15). Nevertheless, these commercially well-developed batteries show drawbacks of poor cycle stability (nickel-metal hydrides), high cost (nickel-hydrogen), or environmental footprint (nickel-cadmium) (16–18). A 30% potassium hydroxide (KOH) solution is used as the electrolyte. The steel vessel is equipped with a gas inlet and outlet to get rid of air and to direct the hydrogen flow into and out of the cell when necessary. A prototypical Ni-H testing cell is shown in *SI Appendix, Fig. S1*. During charge, the cathode $\text{Ni}(\text{OH})_2$ is oxidized to NiOOH ; meanwhile hydrogen gas is evolved from alkaline electrolyte on the anode via the NiMoCo-catalyzed HER. During discharge, the cathode NiOOH is reduced back to $\text{Ni}(\text{OH})_2$ and hydrogen gas is oxidized on the anode via the NiMoCo-catalyzed HOR. The redox reactions of the Ni-H battery during charge and discharge can be described as:

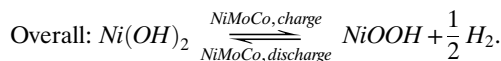
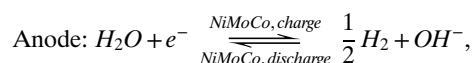
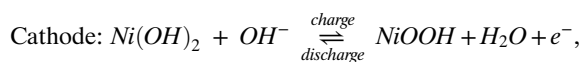


Fig. 1B illustrates the electrode configuration and specification of the Ni-H battery. The cathode was made by heavily coating micrometer-sized $\text{Ni}(\text{OH})_2$ spheres (Fig. 1C, *Inset*) into nickel foam to form a compact electrode (*SI Appendix, Fig. S2*) (19). Scanning electron microscopy (SEM) images show that the $\text{Ni}(\text{OH})_2$ cathode has an average thickness of $\sim 700 \mu\text{m}$ (Fig. 1C). Due to the high density of the $\text{Ni}(\text{OH})_2$ microspheres, the tap density of the cathode is $\sim 2.6 \text{ g cm}^{-3}$, corresponding to a high mass loading of $\sim 182 \text{ mg cm}^{-2}$. The $\text{Ni}(\text{OH})_2$ was further characterized by X-ray diffraction (XRD) to be β -phase (*SI Appendix, Fig. S3*), which was known as the most stable phase in the $\text{Ni}(\text{OH})_2$ family (16). The large thickness, high mass loading, and tap density of the $\text{Ni}(\text{OH})_2$ electrode are among that of industry levels, enabling our Ni-H battery into practical energy storage applications. In contrast, the anode comprises a 3D thin layer of NiMoCo catalyst, which was directly grown on porous nickel foam without any conducting additive or binder (Fig. 1B). XRD confirmed the crystal phase of the NiMoCo alloy (*SI Appendix, Fig. S4*). High-resolution SEM images reveal that the NiMoCo consists

of many interconnected nanoparticles (Fig. 1D, *Inset*). It is further disclosed by transmission electron microscopy that the NiMoCo nanoparticles are in the range of tens of nanometers (*SI Appendix, Fig. S5*). The scanning transmission electron microscopy and the elemental mapping of the NiMoCo alloy clearly demonstrate the uniform distribution of the individual elements of Ni, Mo, and Co (*SI Appendix, Fig. S6*). The developed NiMoCo electrode has some unique features to the Ni-H battery. (i) Due to the 3D characteristic of the nickel foam, the resulting NiMoCo electrode retains the macroporous hierarchical nature (Fig. 1D). Meanwhile, the interconnected NiMoCo nanoparticles give rise to the formation of nanopores in between, making a porous NiMoCo electrode with highly accessible surface for fast battery charge and discharge reactions. (ii) The generated hydrogen gas can be easily evolved on the porous anode in the charge process and be effectively oxidized in the discharge process. (iii) The nickel foam skeletons are interconnected virtually free-of-junction, assuring high electrical conductivity of the electrodes for good battery operation.

Fig. 2 demonstrates the electrochemical performance of the Ni-H cylindrical battery using the compact Ni(OH)₂ cathode and 3D NiMoCo anode. The galvanostatic charge and discharge tests at a constant current of 50 mA ($\sim 2.78 \text{ mA cm}^{-2}$) represent distinct charge and discharge plateaus around 1.55 and 1.25 V, respectively (Fig. 2A, *Inset*), which agree well with the reaction potentials between Ni(OH)₂/NiOOH and HER/HOR (17). Our Ni-H cylindrical battery can achieve high discharge capacity of 640 mAh, corresponding to Coulombic efficiency of $\sim 98.5\%$, which is equivalent to a specific capacity of 195 mAh g^{-1} [based on the mass of Ni(OH)₂] and areal capacity of 35.5 mAh cm^{-2} . The Ni-H battery under different current densities shows well-retained discharge capacities, demonstrating its remarkable rate capability (Fig. 2A), although it shows gradually increased charge–discharge overpotentials and slightly decreased Coulombic efficiencies with the increase of charge

currents (Fig. 2A, *Inset*). For example, the discharge capacity of the Ni-H battery at current density of 120 mA is still as high as $\sim 618 \text{ mAh}$ with the Coulombic efficiency of $\sim 95\%$. Meanwhile, our Ni-H battery can be operated under fast charge mode. A set of the charge–discharge measurements shows that the discharge capacities of the Ni-H battery at current density of 50 mA stayed almost the same under different charge-current densities (from 50 to 150 mA) (*SI Appendix, Fig. S7*). Impressively, the Ni-H battery exhibits excellent rechargeability, retaining above 95% of the charge capacity (Fig. 2B) and Coulombic efficiency (*SI Appendix, Fig. S8*) after 600 cycles at a current of 100 mA ($\sim 5.56 \text{ mA cm}^{-2}$). The energy density of our Ni-H cylindrical battery is calculated to be $\sim 140 \text{ Wh kg}^{-1}$ (normalized to the mass of all components in the cell but excluding the steel vessel). On the basis of the electrochemical performance, the energy cost of the materials utilization in the Ni-H cylindrical battery is estimated to be $\sim \$83 \text{ kWh}^{-1}$, showing promise for the DOE cost target of $\$100 \text{ kWh}^{-1}$ for large-scale energy storage applications (*SI Appendix, Table S1*). Notably, the capital cost of the Ni-H system can be further reduced by optimization of the electrode materials and the battery operation system.

The outstanding electrochemical performance of the Ni-H battery is largely ascribed to the electrocatalytic properties of the NiMoCo anode toward both HER and HOR. Over the past few decades, tremendous efforts have been devoted to the development of low-cost, highly active hydrogen catalysts for HER and HOR (20–24). The state-of-the-art HER electrocatalysts include precious metals (Pt, Ir, Pd) (25), sulfides (MoS₂, NiS₂) (26, 27), phosphide (28), carbide (29), nitride (30), metal alloys (31), and metal-free materials (32). The mostly investigated HOR electrocatalysts are precious metals (Pt, Ir, Ru, Pd) (20, 25). However, only a few catalysts showed bifunctional HER/HOR activities, among which Pt is considered as one of the most active catalysts. Therefore, it is important to develop low-cost alternatives to

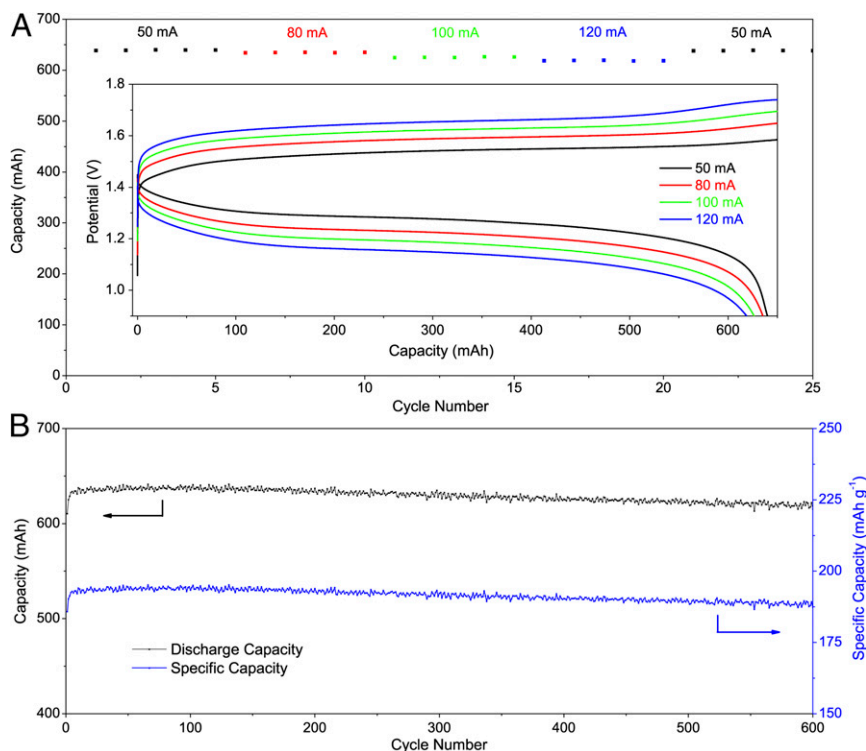


Fig. 2. Electrochemical performance of the Ni-H cylindrical battery. (A) The rate capability of the Ni-H battery. (*Inset*) Galvanostatic charge–discharge curves of the cell at different currents. (B) Cycle stability of the cell at a constant current of 100 mA.

replace the costly Pt. There are few reports on the fabrication of low-cost bifunctional electrocatalysts for both HER and HOR to date. We studied the electrocatalytic performance of the NiMoCo alloy as bifunctional hydrogen electrode for HER/HOR. In fact, NiMo has been recognized as a very active HER catalyst in alkaline media previously (33, 34). Recently, it was found that NiMoCo with a small amount of Co substitution showed comparable HOR activity to that of Pt due to its optimal hydrogen binding energy (22). The HER activity of the catalyst was tested in a typical three-electrode configuration. The nickel foam substrate and Pt/C-coated nickel foam are included for comparison. As shown in Fig. 3A, the Pt/C and NiMoCo electrodes exhibit significantly higher current densities than that of the nickel foam, indicating the negligible HER activity of the

nickel foam and significant activity of the Pt/C and NiMoCo catalysts. The exceptional HER activity of NiMoCo approaches the benchmark Pt/C catalyst. It requires overpotential of only ~ 80 mV for the NiMoCo electrode to drive hydrogen generation at current density of 10 mA cm^{-2} , which is highly comparable to that of the Pt/C catalyst which has overpotential of ~ 71 mV. To reach a high current density of 200 mA cm^{-2} , the applied overpotential of the NiMoCo electrode is as low as ~ 180 mV, making it one of the most active nonprecious electrocatalysts toward HER in alkaline solutions (35–37). Remarkably, the NiMoCo demonstrates outstanding long-term stability, showing no noticeable HER activity degradation over 1,500 h of hydrolysis at current density of 20 mA cm^{-2} (Fig. 3C). As comparison, the Pt/C catalyst shows gradual activity degradation over 800 h of

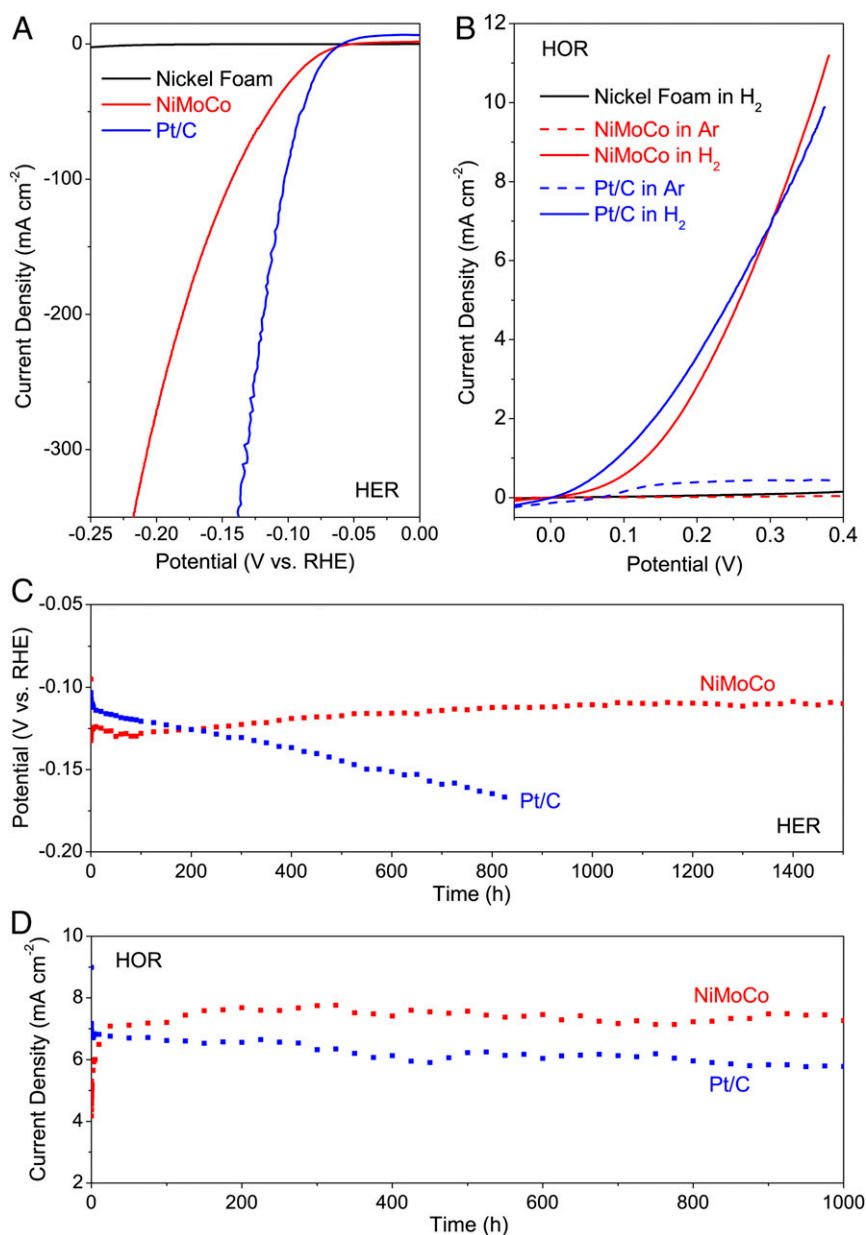


Fig. 3. Electrochemical performance of the bifunctional NiMoCo electrode for HER/HOR. (A) HER polarization curves of nickel foam, NiMoCo, and Pt/C on nickel foam. (B) HOR polarization curves of nickel foam, NiMoCo, and Pt/C on nickel foam under Ar and H_2 atmospheres. (C) Chronopotentiometric stability tests of the NiMoCo and Pt/C electrodes under constant current density of 20 mA cm^{-2} . The HER tests were performed in a three-electrode setup in the electrolyte of 30% KOH. (D) Chronoamperometric stability tests of the NiMoCo and Pt/C electrodes at constant potential of 0.3 V. The HOR tests were conducted in a two-electrode setup under H_2 atmosphere in the electrolyte of 30% KOH.

hydrolysis, probably due to the detachment of the Pt/C from the nickel foam which is caused by the generous hydrogen evolution bubbles.

We then applied a two-electrode setup to test the long-term HOR activity of the catalysts. Fig. 3B shows the polarization curves of the nickel foam, Pt/C, and NiMoCo on nickel foam under different gas conditions. The anodic current above zero is an indicator of hydrogen oxidation. It shows that the Pt/C and NiMoCo have negligible activities toward HOR under argon atmosphere, virtually because of the limited availability of hydrogen gas in the testing cell. Nickel foam shows no detectable HOR activity under hydrogen atmosphere. In comparison, both Pt/C and NiMoCo exhibit the typical polarization curves with large current densities under hydrogen atmosphere, indicating their excellent HOR activities. The NiMoCo electrode was tested to have an onset potential of 0 V toward HOR, which is the same as that of the Pt/C electrode, confirming its active HOR catalytic performance. We have also performed long-term stability tests toward the HOR activity of the NiMoCo electrode. Impressively, the NiMoCo electrode shows negligible activity degradation over 1,000 h of consecutive hydrogen oxidation (Fig. 3D). In contrast, the Pt/C electrode shows slight activity decay over long term (Fig. 3D). The outstanding HER/HOR activities of the NiMoCo electrode make it an exceptional bifunctional hydrogen catalyst for the Ni-H battery application.

The development of the NiMoCo catalyst as the 3D hydrogen electrode provides many advantages over the conventional slurry-coated Pt/C catalysts. (i) Compared with the costly Pt/C, the use of low-cost NiMoCo as the hydrogen catalyst can dramatically reduce the battery cost, making it highly promising for large-scale energy storage application. (ii) The electrochemical deposition of the NiMoCo catalyst on nickel foam gives rise to a 3D electrode with no carbon additive or polymer binder, which not only improves the electrode conductivity but also avoids the carbon oxidation induced catalyst failure or the possible catalytic

poisons (38). (iii) The dc power supplied two-electrode deposition is of large-scale fabrication (SI Appendix, Fig. S9), allowing the development of the Ni-H battery for large-scale applications. (iv) The electrodeposition of NiMoCo is applicable to any conductive substrates. In this regard, we have successfully deposited the NiMoCo alloys onto nickel foam and foil, stainless-steel mesh and foil, and carbon fiber cloth (SI Appendix, Fig. S10). (v) The composition, morphology, and thickness of the NiMoCo can be well controlled by the electrodeposition, which provides a general approach to the optimization of the NiMoCo catalyst and to the fabrication of other metal/metal alloys for many widespread applications.

We developed small-sized Swagelok battery to further investigate the electrochemical performance of the Ni-H battery (SI Appendix, Fig. S11). The Ni(OH)₂ cathode, separator, and the NiMoCo- or Pt/C-catalyzed hydrogen anode are laminated in stacks for the assembly of the Swagelok Ni-H battery. The galvanostatic charge–discharge curves of the Swagelok Ni-H battery by the deployments of the NiMoCo and Pt/C anodes (denoted as Ni-NiMoCo and Ni-Pt batteries) demonstrate the comparable electrochemical behaviors (Fig. 4A). Specifically, the charge potential of the Ni-Pt battery is slightly lower than that of the Ni-NiMoCo battery (Fig. 4A), which is consistent with the HER behaviors of the Pt/C and NiMoCo anodes (Fig. 3A). However, the Ni-NiMoCo battery shows better discharge characteristics in terms of a slightly higher discharge potential and thus discharge capacity. Impressively, the Swagelok Ni-NiMoCo battery has outstanding long-term cycle stability, exhibiting negligible capacity decay over 1,500 cycles (Fig. 4B). However, the Ni-Pt battery shows gradual capacity degradation over cycling, which is probably due to the partial detachment of the Pt/C catalyst from the anode during the intensive HER/HOR in the long cycling tests. The electrochemical performance of the Ni-NiMoCo battery demonstrates the remarkable electrocatalytic activity of

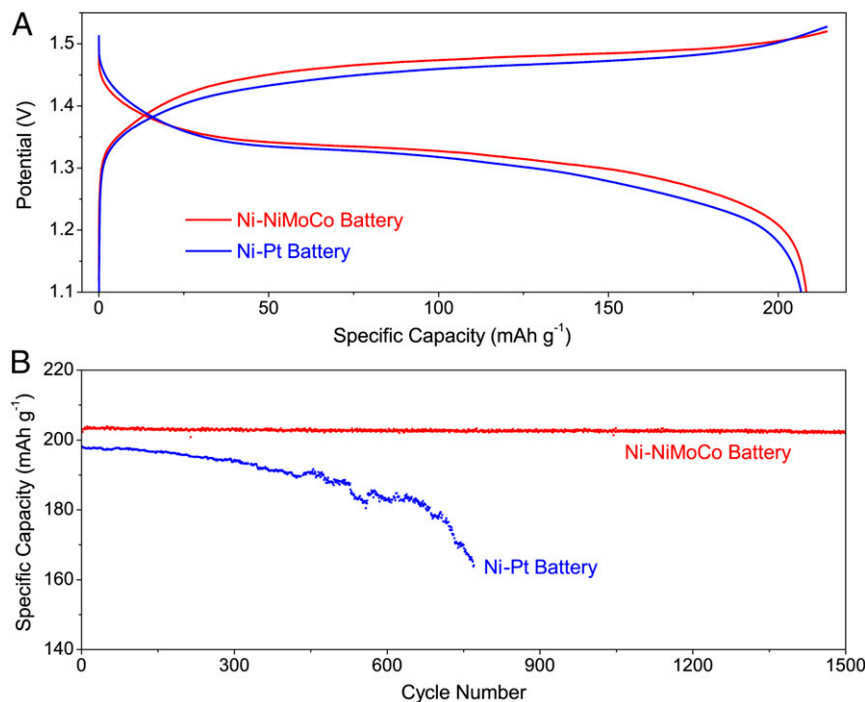


Fig. 4. The Ni-H Swagelok battery. (A) Galvanostatic charge–discharge curves of the Swagelok Ni-NiMoCo and Ni-Pt batteries under current density of 5 mA cm⁻². (B) Long-term cycle stability behaviors of the Ni-NiMoCo and Ni-Pt batteries at current density of 10 mA cm⁻². The Ni-H Swagelok batteries were fabricated using the Ni(OH)₂ cathode, the Pt/C or NiMoCo anode in 30% KOH electrolyte.

the NiMoCo electrode as a robust bifunctional HER/HOR catalyst in the alkaline electrolyte.

In conclusion, we have developed a Ni-H battery using Ni(OH)₂ cathode and a low-cost NiMoCo-catalyzed HER/HOR anode. The Ni-H battery shows energy density of ~140 Wh kg⁻¹ (based on active materials) with excellent rechargeability over 1,500 cycles. The low energy cost of ~\$83 kWh⁻¹ based on active materials achieves the DOE target of \$100 kWh⁻¹, which makes it promising for the large-scale energy storage application. Future work will be focused on the optimization of the electrode

materials and the battery systems for improved electrochemical performance. The battery chemistry demonstrated in the present work may lead to the exploration of next-generation, low-cost rechargeable batteries.

ACKNOWLEDGMENTS. We thank D. S. Kong, K. Yan, Y. C. Qiu, G. D. Li, J. S. Lee, and G. X. Chen for fruitful discussions on experiments. We also thank T. Hymel, Y. Li, and A. Pei for discussions and comments on the manuscript. This work was supported by the DOE, Office of Basic Energy Sciences, Materials Sciences and Engineering Division, under Contract DE-AC02-76-SFO0515.

1. Chu S, Majumdar A (2012) Opportunities and challenges for a sustainable energy future. *Nature* 488:294–303.
2. Yang Z, et al. (2011) Electrochemical energy storage for green grid. *Chem Rev* 111: 3577–3613.
3. Dunn B, Kamath H, Tarascon JM (2011) Electrical energy storage for the grid: A battery of choices. *Science* 334:928–935.
4. Chu S, Cui Y, Liu N (2016) The path towards sustainable energy. *Nat Mater* 16:16–22.
5. Wang K, et al. (2014) Lithium-antimony-lead liquid metal battery for grid-level energy storage. *Nature* 514:348–350.
6. Rehman S, Al-Hadhrani LM, Alam MM (2015) Pumped hydro energy storage system: A technological review. *Renew Sustain Energy Rev* 44:586–598.
7. Chen HS, et al. (2009) Progress in electrical energy storage system: A critical review. *Prog Nat Sci* 19:291–312.
8. Pavlov D (2011) *Lead-Acid Batteries: Science and Technology: A Handbook of Lead-Acid Battery Technology and Its Influence on the Product* (Elsevier Science, Amsterdam), pp 1–643.
9. Noack J, Roznyatovskaya N, Herr T, Fischer P (2015) The chemistry of redox-flow batteries. *Angew Chem Int Ed Engl* 54:9776–9809.
10. Goodenough JB, Kim Y (2010) Challenges for rechargeable Li batteries. *Chem Mater* 22:587–603.
11. Oshima T, Kajita M, Okuno A (2004) Development of sodium-sulfur batteries. *Int J Appl Ceram Technol* 1:269–276.
12. Kim H, et al. (2013) Liquid metal batteries: Past, present, and future. *Chem Rev* 113: 2075–2099.
13. Zimmerman A (2008) *Nickel-Hydrogen Batteries: Principles and Practice* (Aerospace Press, El Segundo, CA).
14. Pan HL, Hu YS, Chen LQ (2013) Room-temperature stationary sodium-ion batteries for large-scale electric energy storage. *Energy Environ Sci* 6:2338–2360.
15. Dell RM (2000) Batteries—Fifty years of materials development. *Solid State Ion* 134: 139–158.
16. Shukla AK, Venugopalan S, Hariprakash B (2001) Nickel-based rechargeable batteries. *J Power Sources* 100:125–148.
17. Lackner JL, McCoy DA (1986) Investigation of nickel-hydrogen battery technology for the radarsat spacecraft. *J Power Sources* 18:259–264.
18. Beck F, Rüetschi P (2000) Rechargeable batteries with aqueous electrolytes. *Electrochim Acta* 45:2467–2482.
19. Ogasawara T, et al. (1999) US Patent US6849359B1.
20. Sheng WC, Gasteiger HA, Shao-Horn Y (2010) Hydrogen oxidation and evolution reaction kinetics on platinum: Acid vs alkaline electrolytes. *J Electrochem Soc* 157: B1529–B1536.
21. Skulason E, et al. (2010) Modeling the electrochemical hydrogen oxidation and evolution reactions on the basis of density functional theory calculations. *J Phys Chem C* 114:18182–18197.
22. Sheng WC, et al. (2014) Non-precious metal electrocatalysts with high activity for hydrogen oxidation reaction in alkaline electrolytes. *Energy Environ Sci* 7:1719–1724.
23. Zou X, Zhang Y (2015) Noble metal-free hydrogen evolution catalysts for water splitting. *Chem Soc Rev* 44:5148–5180.
24. Strmcnik D, et al. (2013) Improving the hydrogen oxidation reaction rate by promotion of hydroxyl adsorption. *Nat Chem* 5:300–306.
25. Durst J, et al. (2014) New insights into the electrochemical hydrogen oxidation and evolution reaction mechanism. *Energy Environ Sci* 7:2255–2260.
26. Kong DS, Cha JJ, Wang HT, Lee HR, Cui Y (2013) First-row transition metal dichalcogenide catalysts for hydrogen evolution reaction. *Energy Environ Sci* 6:3553–3558.
27. Li Y, et al. (2011) MoS₂ nanoparticles grown on graphene: An advanced catalyst for the hydrogen evolution reaction. *J Am Chem Soc* 133:7296–7299.
28. Shi Y, Zhang B (2016) Recent advances in transition metal phosphide nanomaterials: Synthesis and applications in hydrogen evolution reaction. *Chem Soc Rev* 45: 1529–1541.
29. Liao L, et al. (2014) A nanoporous molybdenum carbide nanowire as an electrocatalyst for hydrogen evolution reaction. *Energy Environ Sci* 7:387–392.
30. Cao B, Veith GM, Neuefeind JC, Adzic RR, Khalifah PG (2013) Mixed close-packed cobalt molybdenum nitrides as non-noble metal electrocatalysts for the hydrogen evolution reaction. *J Am Chem Soc* 135:19186–19192.
31. Birry L, Lasia A (2004) Studies of the hydrogen evolution reaction on Raney nickel-molybdenum electrodes. *J Appl Electrochem* 34:735–749.
32. Zhang J, et al. (2016) N,P-codoped carbon networks as efficient metal-free bifunctional catalysts for oxygen reduction and hydrogen evolution reactions. *Angew Chem Int Ed Engl* 55:2230–2234.
33. Fan CL, Piron DL, Slebo A, Paradis P (1994) Study of electrodeposited nickel-molybdenum, nickel-tungsten, cobalt-molybdenum, and cobalt-tungsten as hydrogen electrodes in alkaline water electrolysis. *J Electrochem Soc* 141:382–387.
34. McKone JR, Sadtler BF, Werlang CA, Lewis NS, Gray HB (2013) Ni-Mo nanopowders for efficient electrochemical hydrogen evolution. *ACS Catal* 3:166–169.
35. Gong M, et al. (2014) Nanoscale nickel oxide/nickel heterostructures for active hydrogen evolution electrocatalysis. *Nat Commun* 5:4695.
36. Greeley J, Jaramillo TF, Bonde J, Chorkendorff IB, Nørskov JK (2006) Computational high-throughput screening of electrocatalytic materials for hydrogen evolution. *Nat Mater* 5:909–913.
37. Wang HT, et al. (2015) Bifunctional non-noble metal oxide nanoparticle electrocatalysts through lithium-induced conversion for overall water splitting. *Nat Comm* 6:7261.
38. Shao YY, Liu J, Wang Y, Lin YH (2009) Novel catalyst support materials for PEM fuel cells: Current status and future prospects. *J Mater Chem* 19:46–59.